

VARIATION OF THE REFRACTIVE INDEX OF LIQUIDS AND GLASSES IN A HIGH INTENSITY FIELD OF A RUBY LASER

A. P. VEDUTA and B. P. KIRSANOV

P. N. Lebedev Physics Institute, Academy of Sciences, USSR

Submitted December 26, 1967

Zh. Eksp. Teor. Fiz. 54, 1374-1379 (May, 1968)

Interference methods are used to measure the χ_3^{1111} and χ_3^{1122} components of the nonlinear susceptibility tensor in a single experiment with a satisfactory relative accuracy. Since the results of measurements are not consistent with the purely orientational concept of the mechanism responsible for the nonlinearity, it is suggested that other mechanisms such as that of an electronic nature play a significant role in the investigated phenomenon. This is further confirmed by theory and experiments designed to investigate the variation of the dielectric constant of materials in a variable field.

PULSED lasers today can readily produce directed light beams with intensities of the order of 10^8-10^9 W/cm². The conditions of propagation of such beams in transparent media significantly depend on the nonlinear properties of the media. As an example we note the self-focusing phenomenon^[1,2] that is due to the dependence of the refractive index on the intensity of the transmitted light wave.

In media with symmetry inversion the variation of the refractive index depends on the third order nonlinear polarization of the electric field intensity^[3]. If the frequency of the high intensity field coincides with the frequency used in the measurement (weak field) we have

$$\delta n_{\parallel} = \frac{2\pi}{n} \cdot 3\chi_3^{1111} |E(\omega)|^2, \quad \delta n_{\perp} = \frac{2\pi}{n} \cdot 3\chi_3^{1122} |E(\omega)|^2, \quad (1)$$

$$\chi_3^{1111} = \chi_3^{1222} + \chi_3^{1221} + \chi_3^{1212}, \quad \chi_3^{1212} = \chi_3^{1221}.$$

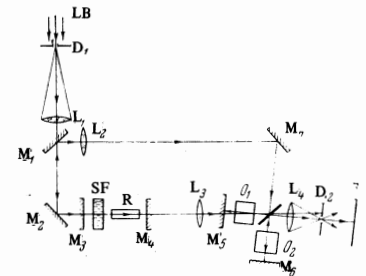
Here χ_3^{ijkl} are components of the nonlinear susceptibility tensor of the fourth rank (see (1) in^[3]), $E(\omega)$ is the intensity of the strong electric field, n is the refractive index of the medium at the frequency ω , and δn_{\parallel} and δn_{\perp} are the variations of the refractive index for the cases of parallel and perpendicular mutual orientations of the strong and weak field polarizations.

According to the current theory the principal mechanism responsible for the variation of the refractive index is the orientation of anisotropically polarized molecules^[3,4]. This theory is supported by the fact that the relationship

$$\eta = \chi_3^{1221} / (\chi_3^{1122} + \chi_3^{1212}), \quad (2)$$

based on currently available experimental results yields a value close to $\eta = 3$ which follows from the orientation theory^[3,5]. The components χ_3^{1221} and χ_3^{1212} of this relationship were measured experimentally for certain liquids in terms of the rotation of the polarization ellipse and the magnitude of birefringence induced by the high intensity field^[6-8]. The magnitude of the χ_3^{1122} component was determined from χ_3^{1111} which in turn was evaluated from the self-focusing threshold. Thus (2) contains quantities determined from various experiments with a low absolute measurement accuracy (about 50%). For example, there is a significant difference between the results obtained in^[6] and^[7]. Furthermore, the validity of determining χ_3^{1111} from the self-focusing threshold is

FIG. 1. Optical diagram for the measurement of χ_3^{1111} (designations in text).



doubtful since a full explanation of the self-focusing phenomenon is not yet available. There are liquids for which the value of η determined by this method is 1.5 and even 1.0 rather than 3. Hence it follows that the available experimental results do not yet permit us to draw unambiguous conclusions concerning the mechanism of variation of the refractive index.

In the present work interference methods were used to perform direct measurements of the χ_3^{1111} and χ_3^{1122} components in a single experiment yielding a satisfactory relative accuracy. The obtained results are not consistent with the concept of a nonlinearity mechanism that is based on molecular orientation only. We thus propose that along with this mechanism others may also play a significant role in this phenomenon, such as the electron mechanism whose relevance is further supported by theory.

THE EXPERIMENT AND THE RESULTS

The optical setup for absolute measurements of δn_{\parallel} is shown in Fig. 1. We used a pulsed ruby oscillator with saturable filter consisting of mirrors M_3 and M_4 , rod R , and saturable filter SF . The oscillator output emitted through an opening in mirror M_5 was focused by lens L_3 with a focal length of 25 cm within the investigated object O_1 (strong field).

The investigated specimen was placed in one of the arms of a Michelson interferometer formed by mirrors M_5 and M_6 and the splitter plate. The measuring beam (weak field) used to photograph the interference patterns was represented by the emission of the same oscillator emerging from fixed mirror M_3 and directed to the interferometer by mirrors M_2 , M_1 , and M_7 . The delay

of the measuring pulse caused by the geometry of the system was 2–3 nsec. Lens L_2 was used to compensate for the angular divergence of the measuring beam. The ratio of intensities of the strong to the weak fields at the interaction site was of the order of 10^3 .

The interference pattern was projected on film F by lens L_4 . To block the strong field from fogging the film the longitudinal axis of the interferometer was inclined to the beam axis by a small angle ($\sim 3^\circ$) and diaphragm D_2 was inserted in the focus of L_4 to admit only the measuring beam. The entire system was aligned with light beam LB of a He-Ne laser that was additionally collimated with diaphragm D_1 and lens L_1 .

The power density of the strong field was measured locally at the site of the specimen through a 1 mm diaphragm according to a method described in^[9]. The light beam diameter at this point was about 3 mm and occupied merely a portion of the interference field. The inhomogeneity of field intensity distribution over the generation disc limited the absolute accuracy of measurement of δn_{\parallel} . In our case the accuracy was $\sim 50\%$.

The maximum power averaged over the generation disc and measured in this manner in the interaction region was 350 MW/cm^2 ; this value was well reproducible from pulse to pulse. In order to avoid self-focusing and multiphoton absorption during measurements the maximum power was attenuated to the required level by filters calibrated in the strong field of the same equipment. The effect in liquids was measured in cells 2–10 cm long and rectangular specimens 2–6 cm long were used for measurements in the solid state. In computing δn_{\parallel} we did not use the entire length of the specimen but rather the portion where the strong and weak fields overlapped each other; this was a length of about 4 cm.

Figure 2 shows photographs of interference patterns obtained from the experiment. The arrow shows local distortion of the straight horizontal bands of equal optical paths at the site of field interaction. We could compute δn_{\parallel} from the magnitude of the distortion and knowing the power $P \sim E^2$ we could find χ^{111} from (1).

The results of the measurements are given in the table. The error limits for χ_3^{111} indicated in the table are relative and valid when the results of this work are compared to one another.

In a separate experiment we measured the ratio $\delta n_{\parallel}/\delta n_{\perp} = \chi_3^{111}/\chi_3^{112}$. The experimental setup is shown in Fig. 3. Here R, M_3 , M_4 , and SF are the elements of the pulsed ruby laser used in the preceding experiment. The light beam ($P \approx 50 \text{ MW/cm}^2$) emerging from mirror M_3 was focused on the investigated sample O by the cylindrical lens CL. The sample was placed in the arm of the interferometer consisting of mirrors M_1 , M_2 , and splitter plate SP. The measuring light beam was directed to the interferometer by mirrors M_5 and M_6 . The directions of the weak and the strong light beams were

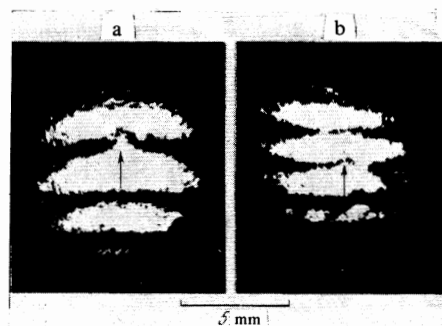


FIG. 2. Examples of interference patterns for the case of absolute measurements of χ_3^{111} . a—o-xylene; b—TF-7 glass.

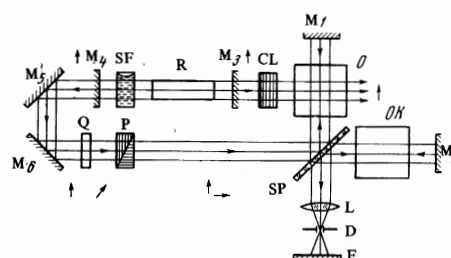


FIG. 3. Optical diagram for measuring the ratio $\chi_3^{111}/\chi_3^{112}$ (designations in text).

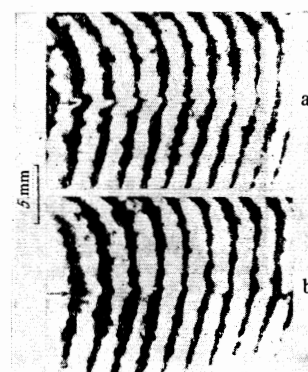


FIG. 4. Examples of interference patterns for quinoline. a— $E_{\text{strong}} \parallel E_{\text{observ}}$; b— $E_{\text{strong}} \perp E_{\text{observ}}$.

mutually perpendicular within the specimen in the field interaction region. The weak field polarization was varied with plate Q of rotating quartz and polaroid P. The interference patterns were photographed in two consecutive generation pulses under the same conditions but with different mutual orientations of polarization: parallel and perpendicular. Figure 4 shows one pair of patterns obtained in this manner.

According to Fig. 4 a bending of the interference bands indicated by arrows can be observed at the site of field interaction. The sought ratio was determined by measuring the magnitude of this bend on each pair of

| Substance | χ_3^{111} 10^{-14} CGSE | $\chi_3^{111}/\chi_3^{112}$ | Substance | χ_3^{111} 10^{-14} CGSE | $\chi_3^{111}/\chi_3^{112}$ |
|--------------|-----------------------------------|-----------------------------|--------------------------|-----------------------------------|-----------------------------|
| Acetone | 18 ± 4 | — | Toluene | 48 ± 5 | 1.40 ± 0.15 |
| Benzene | 37 ± 5 | 1.09 ± 0.20 | Quinoline | 69 ± 7 | 1.28 ± 0.25 |
| Water | 7 ± 3 | — | Ethyl alcohol | 14 ± 3 | — |
| Glycerine | 14 ± 5 | 1.03 ± 0.23 | Ruby (ordinary ray) | ≤ 20 | — |
| Fused quartz | 48 ± 9 | — | Ruby (extraordinary ray) | ≤ 20 | — |
| o-Xylene | 44 ± 9 | 1.24 ± 0.21 | K-8 glass | 15 ± 3 | — |
| Nitrobenzene | 82 ± 10 | 1.41 ± 0.30 | TF-7 glass | 30 ± 7 | 1.02 ± 0.17 |

photographs. The results are given in the table. The error is much lower in this case since the indeterminacy due to the absolute measurements of field distribution is eliminated.

Correct interpretation of the results requires that the experiments be free of macroscopic changes in the medium density due to striction, i.e., that $a \gg v\tau$, where a is the size of the interaction region, v is the velocity of sound in the medium, and τ is the generation pulse length. In our case $a \approx 10^{-1}$ cm, $v \approx 10^5$ – 10^6 cm/sec, and $\tau \approx 10^{-8}$ sec and the above condition is satisfied by a large margin. On the other hand microscopic changes of density, due to self-focusing for example, are not registered in our system because the average medium density in the interaction region remains constant.

The total change of the refractive index is proportional to the integral of the strong field intensity along the interaction length, i.e., to the input power. Hence it follows that the presence of self-focusing should not affect the final result if there are no additional nonlinear effects such as multiphoton absorption. The latter effect can influence the validity of the absolute measurements of χ_3^{1111} . To avoid this in our experiment we used sub-critical input power and cell lengths. We also checked the linear dependence of δn_{\parallel} on power. Under these conditions we observed a saturation of the effect at maximum powers in such media as nitrobenzene and toluene.

DISCUSSION OF RESULTS

The table shows that the ratio $\chi_3^{1111}/\chi_3^{1122}$ determined by the experiment is always positive and corresponds to an increase of the refractive index in both polarizations. This contradicts the orientation mechanism of nonlinearity which calls for a negative ratio¹⁰. Furthermore the observed absolute magnitude of χ_3^{1111} in liquids is of the same order of magnitude as in glasses where orientation is not possible. Consequently orientation seems insignificant also in liquids.

We also attempted to determine experimentally the magnitude of the orientation effects. The experimental setup is shown in Fig. 5. The pulsed ruby laser beam was focused by a cylindrical lens between the plates of a plane capacitor immersed in the investigated medium. The capacitor was charged up to 4 kV. The electrical circuit of the capacitor is shown in Fig. 5 below. Here R_3 and C_b constitute the charging circuit with a large τ . The time constant $C_r R_1$ was of the order of 1 msec. The signal across the load resistor was allowed to enter the input of the oscilloscope whose second beam was impressed with the generation pulse signal from the photomultiplier. The fast reversible change of the dielectric constant δ of the medium due to molecular orientation (the polarizations of the variable and constant fields should be parallel) should produce a short signal across R_1 coinciding with the generation pulse.

We investigated benzene, toluene, and nitrobenzene. The oscilloscopic traces showed a long signal corresponding to the change in δ due to increasing temperature of the medium in the capacitor. The effects due to a change in the magnitude of charge in the capacitor (breakdown and photoeffect) also yield a long signal but of the opposite sign. The length of such signals corresponds to the time constant $C_r R_1$. Short signals however were not observed at any generation pulse power. Using

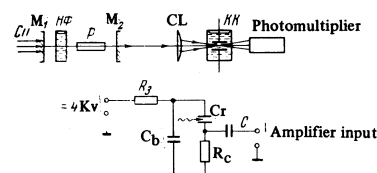


FIG. 5. Setup for the detection of molecular orientation in a variable light field.

the equipment sensitivity, field strength, and the relation between the orientation part of polarization and the dielectric constant¹⁵ we can find the upper limit for the orientation part of χ_3^{ijkl} . This proved to equal $\sim 10^{-15}$ cgs esu, i.e. it was almost by two-three orders of magnitude smaller than the values of χ_3^{1111} given in the table.

We also consider other possible mechanisms. The contribution to χ_3^{ijkl} from the nonlinear electron polarization is proportional to $d^4 N / \hbar^3 \omega^3$, where d is the dipole moment, N is the number of molecules per cm^3 , and ω is the average frequency of optical transitions¹¹. If we consider that the oscillator strengths of the permitted optical transitions equal 0.01–0.1 and that consequently $d \approx (1-3) \times 10^{-18}$ cgs esu then we obtain χ_3^{ijkl} electron $\approx (1-10^2) \times 10^{-14}$ cgs esu for $\omega \approx 10^{15}$ sec^{-1} and $N \approx 10^{22}$ cm^{-3} . A similar computation performed by Faïn¹² also yields the value of 10^{-12} cgs esu for χ_3^{ijkl} electron.

It should be noted that nonlinear electron polarization should also give a signal in a constant field. However in contrast with the orientation mechanism this signal should be approximately two orders of magnitude smaller than that occurring at optical frequencies because of the absence of summed near-resonant frequencies in the denominator of the expression for χ_3^{ijkl} .

In conclusion we give our sincere thanks to M. D. Galanin for useful remarks and discussion.

¹ E. Garmire, R. Y. Chiao, and C. Townes, Phys. Rev. Lett. 16, 347 (1966).

² R. G. Brewer and C. H. Townes, Phys. Rev. Lett. 18, 196 (1967).

³ C. C. Wang, Phys. Rev. 152, 149 (1966).

⁴ R. W. Minck, R. W. Terhune, and C. C. Wang, Proc. IEEE 54, 1357 (1966).

⁵ Y. R. Shen, Phys. Rev. Lett. 20, 378 (1966).

⁶ P. D. Maker, R. W. Terhune, and C. M. Savage, Phys. Rev. Lett. 12, 507 (1964). P. D. Maker and R. W. Terhune, Phys. Rev. 137, A801 (1965).

⁷ P. D. McWane and D. A. Sealer, Appl. Phys. Lett. 8, 278 (1966).

⁸ G. Mayer and F. Gires, Compt. Rend. 258, 2039 (1964).

⁹ A. P. Veduta, ZhETF Pis. Red. 5, 154 (1967) [JETP Lett. 5, 124 (1967)].

¹⁰ Ya. B. Zel'dovich and Yu. P. Raizer, ZhETF Pis. Red. 3, 137 (1966) [JETP Lett. 3, 86 (1966)].

¹¹ V. M. Faïn and Ya. N. Khanin, Kvantovaya radiofizika (Quantum Radiophysics) Sov. Radio, 1965.

¹² V. M. Faïn, Izv. vuzov, Radiofizika 10, 1320 (1967).